Correlation of Antiviral Activity with β-Turn Types for V3 Synthetic Multibranched Peptides from HIV-1 gp120†

Kamel Mabrouk, Jurphaas Van Rietschoten, Hervé Rochat, and Erwann P. Loret*

Laboratoire de Biochimie, CNRS URA 1455, IFR Jean Roche-Faculté de Médecine Nord, 13916 Marseille Cedex 20, France

Received December 14, 1994; Revised Manuscript Received March 7, 1995®

ABSTRACT: SPC3 is a synthetic multibranched peptide containing eight HIV-1 gp120 V3 loop GPGRAF motifs. SPC3 inhibits HIV-1 infection in human lymphocytes and macrophages, while the monomer counterpart of SPC3, i.e., the GPGRAF peptide, has no effect. Circular dichroism (CD) of these molecules in phosphate buffer, pH 7, and in a water solution containing 50% trifluoroethanol (TFE) showed significant differences. In TFE, the inactive monomer has a CD spectrum associated to type II β-turn (class B spectrum), while SPC3 has a class C CD spectrum associated to type I β-turn. To investigate the structure−function relationship, SPC3 analogs were built in solid-phase synthesis, and their activity and structures were compared to SPC3. Analogs having respectively two and four GPGRAF motifs show that polymerization is associated with these structural changes. Analogs with eight motifs but differing in their sequence show also that the sequence is important to stabilize a type I β-turn structure. The activity tests of these analogs show a remarkable correlation between the antiviral activity and their ability to exhibit a class C CD spectrum associated to type I β-turn. Taking in account CD results, a model was made using energy minimization and dynamics, which shows that, for SPC3, a model with motifs in a type I β-turn structure is favored compared to one with a type II β-turn. These data suggest that the SPC3 antiviral activity is related to the structure of the GPGRAF motif in the polymer, with special emphasis on the presence of a type I β-turn structure.

The third variable region (V3) of the HIV-1 surface glycoprotein gp120 is a loop located between two half-cystine residues (Cys-303 and Cys-338) forming a disulfide bridge and is essential for virus infection and tropism (Hwang et al., 1991; Moore & Nara, 1991; Levy, 1993). In infected individuals, most of the neutralizing anti-HIV antibodies are directed against the V3 loop (Moore & Nara, 1991), and many studies aimed to develop a vaccine against HIV infections have been focused on this loop (Bolognesi, 1993). Unfortunately, due to the high variability of this domain, anti-V3 antibodies are type-specific and neutralize, in the best case, only closely related isolates (Javaherian et al., 1990). In order to overcome the problems inherent to envelope variability, V3-loop-related synthetic peptides have been evaluated as potential inhibitors of HIV infection, yet leading to inconsistent results. Occasionally, V3 peptides were found to enhance viral infection (De Rossi et al., 1991). Interestingly, Nehete et al. (1993), using other V3 peptides, observed an inhibition of HIV-1 infection in lymphocytes. Recently, it was reported that a polymer form of the V3 loop consensus motif, Gly-Pro-Gly-Arg-Ala-Phe (GPGRAF) (Larosa et al., 1990), displayed a potent anti-HIV activity *in vitro* while the monomer GPGRAF was inefficient (Fantini et al., 1993; Yahi et al., 1994). Such synthetic polymeric constructions (SPCs), consisting of an uncharged poly-Lys core matrix (which accounts for about 15% of the total weight), have been used in the past as immunogens (Tam, 1988) and, in the case of the HIV-1 V3 loop, elicited type-specific responses (Nardelli et al., 1992).

The aim of this study was to determine an eventual correlation between structures and the antiviral activity of the GPGRAF sequence in SPC3. Circular dichroism (CD) and modeling were used to get structural information, and the assay of HIV-1-induced syncytia formation was the test of antiviral activity. Our results show that GPGRAF adopts two different structures as monomer and as SPC. In trifluoroethanol, these structures are identified as being a type II β-turn for the monomer form and a type I β-turn for the SPC form. Using a panel of SPC3 analogs, we show that a type I β-turn structure is associated with an antiviral activity. Furthermore, the SPC3 modeling shows that when the SPC3 motifs have a type II β-turn structure, there is a high-energy model, and the type II β-turns disappeared after energy minimization while the structure with the SPC3 motifs in the type I β-turn structure is stable and leads to a low-energy structure after energy minimization.

MATERIALS AND METHODS

Peptide Synthesis. The nomenclature used for SPCs gives the peptide sequence in brackets, followed by the index of polymerization and the term SPC. For instance, $[GPGRAF]_8$-SPC means a SPC containing eight GPGRAF motifs, i.e., $(GPGRAF)_8$-$(K)_4$-$(K)_2$-K-βA. This particular multibranched peptide, based on the consensus sequence of the HIV-1 V3 loop obtained from LaRosa et al. (1990), was also referred to as SPC3. Chemical synthesis of peptides was performed by the solid-phase technique (Merrifield, 1986). The peptide chains were elongated stepwise on 4-(oxymethyl)-PAM resin using optimized *tert*-butyloxycarbonyl/benzyl chemistry, as previously described (Sabatier et al., 1993). Amino acid

† Financial support from CNRS is gratefully acknowledged.

* To whom correspondence should be addressed: Institut de Biologie Structurale et Microbiologie, LIDSM, CNRS UPR 9027, 31 Chemin Joseph Aiguier, 13402 Marseille Cedex 20, France.

® Abstract published in *Advance ACS Abstracts,* June 1, 1995.

0006-2960/95/0434-8294$09.00/0

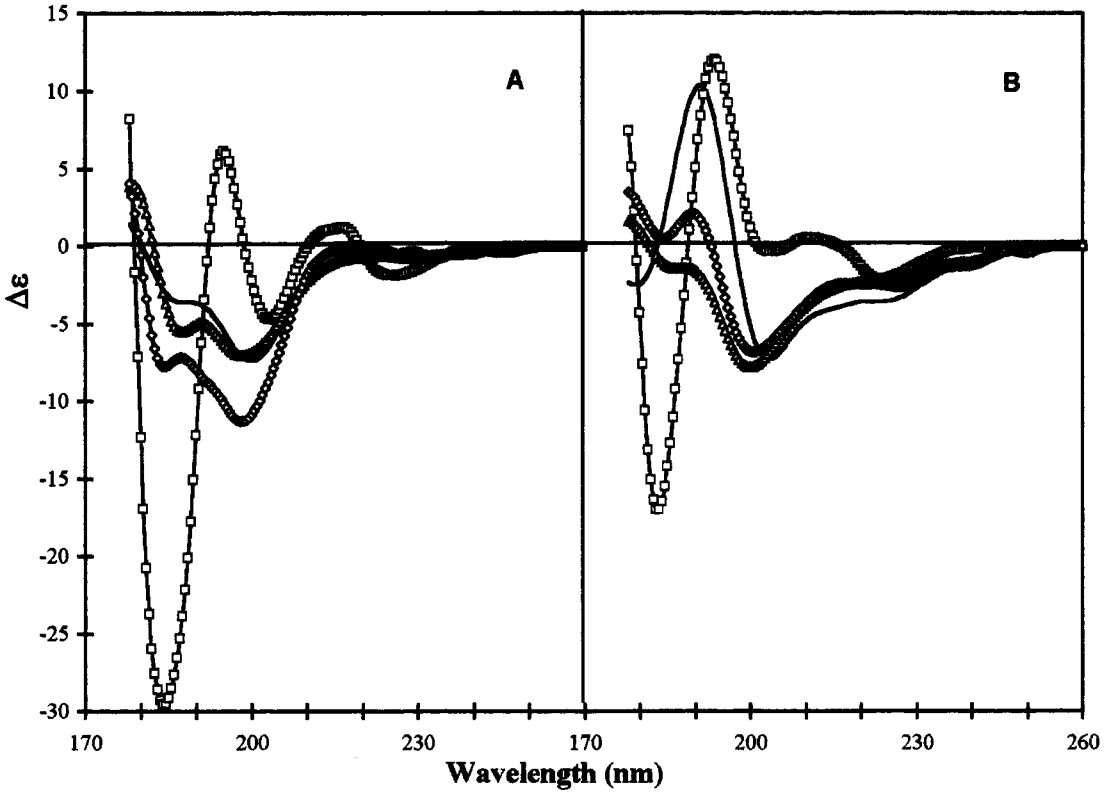

FIGURE 1: CD spectra of GPGRAF (square), $[GPGRAF]_2$-SPC (triangle), $[GPGRAF]_4$-SPC (diamond), and $[GPGRAF]_8$-SPC or SPC3 (solid line) in 20 mM phosphate buffer, pH 7 (panel A), and in a water solution containing 50% trifluoroethanol (panel B).

analysis of the purified SPCs agreed with the deduced amino acid ratios. SPC3 was further characterized by electrospray mass spectrometry (experimental M_r = 5671.1; deduced M_r = 5671.6). Stock solutions of peptides (10^{-3} M) were filter-sterilized on 0.22-μm low protein binding membranes (Costar) and stored as aliquot at −20 °C prior to use.

Cell Culture. Human peripheral blood mononuclear cells (PBMCs) were obtained from a healthy donor, activated with phytohemagglutinin (PHA, Sigma), and cultivated in RPMI 1640 containing 10% fetal calf serum with interleukin-2 (Biotest) (complete medium), as described previously (Yahi et al., 1992). Human T-lymphoblastoid cells were routinely grown in RPMI 1640 supplemented with 10% fetal calf serum.

Assay of HIV-1-Induced Syncytia Formation. A total of 5×10^4 8E5 cells chronically infected with a reverse transcriptase (RT) deficient HIV-1 (IIIB) isolate (Folks et al., 1985) were cocultivated with 15×10^4 PHA-stimulated PBMCs in the presence of the indicated peptide in 96-well microplates, as described (Hildreth & Orentas, 1989). Syncytia formation was determined after 24 h of incubation in the continued presence of the peptides.

CD Measurements. For UV−CD measurements, the samples were in 20 mM phosphate buffer (pH 7) or in a water solution containing 50% trifluoroethanol (TFE). CD spectra were measured in 50-μm path-length cells from 260 to 178 nm with a JOBIN-YVON (Long-Jumeau, France) UV−CD spectrophotometer. Measurements were performed at 20 °C. CD spectra are reported as $\Delta\epsilon$ per amide. Synthetic peptides were analyzed for amino acid content, and the concentration was determined on a Beckman amino acid analyzer. Peptide concentrations were in a range of 0.5−1 mg/mL. Light transmission of samples in the far-UV (down to 175 nm) was checked with a SAFAS (Monaco) spectrophotometer.

Molecular Models. Models were build with the Insight II and Discover softwares from BIOSYM Technologies, Inc. (San Diego, CA), running on a Silicon Graphics XS 24 R3000 Indigo Workstation. The structures were optimized with the CVFF force field in terms of the internal energies, using the van der Waals energy to monitor each step of the modeling. The pH was set up at 7. Minimization was performed with steepest descent, conjugate gradient, and quasi Newton Raphton algorithms with a maximum derivative of 0.1 kcal/Å in the final steps. Dynamic steps were performed at 300 K for 10 ps. The ligand-design study was performed with the LUDI software from BIOSYM Technologies, Inc.

RESULTS AND DISCUSSION

SPC3, a synthetic multibranched peptide containing eight GPGRAF motifs, inhibits HIV-1 infection of human lymphocytes and macrophages, while the monomer counterpart of SPC3, i.e., the peptide GPGRAF, has no antiviral activity (Fantini et al., 1993). Starting from these results, we investigated by circular dichroism (CD) possible structural changes due to either the polymerization or the sequence. The CD spectra were made in phosphate buffer, pH 7, and in a water solution containing 50% trifluoroethanol (TFE) considered to mimic conditions found near the lipid membranes (Urry, 1972).

CD spectra of SPC3, the GPGRAF monomer, and SPC analogs with two and four motifs are shown in phosphate buffer, pH 7 (Figure 1A), and in TFE (Figure 1B). In these two environments, the GPGRAF monomer and SPC3 CD spectra are different. In TFE, the monomer shows a class

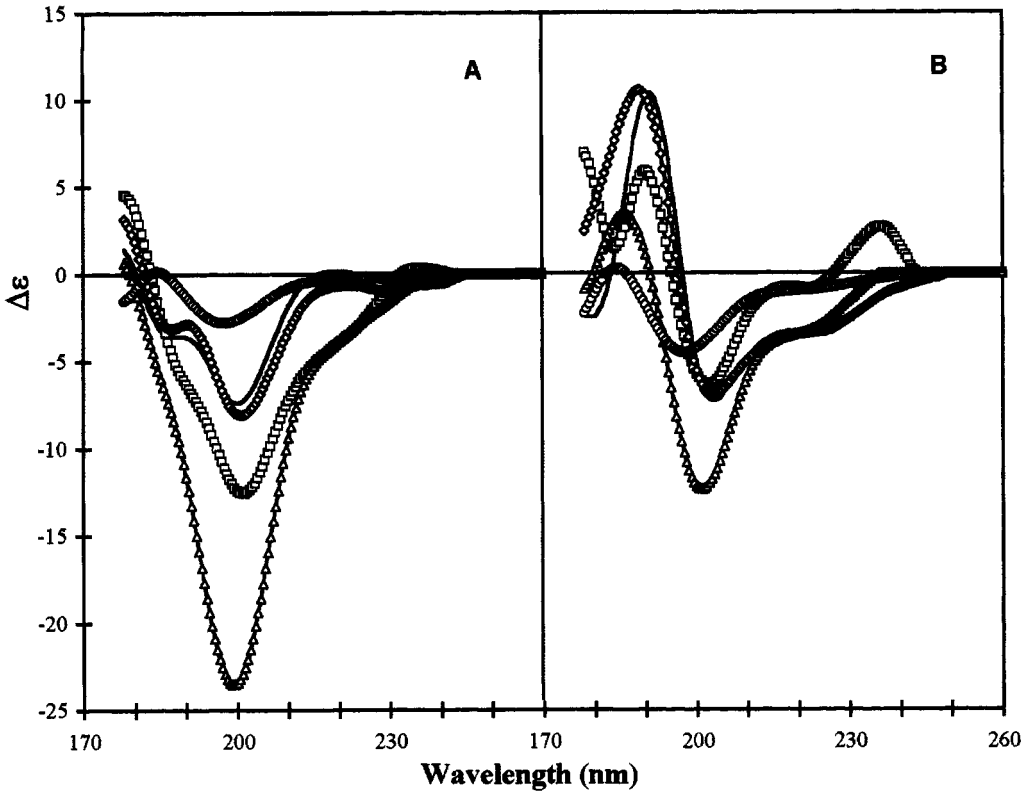

FIGURE 2: CD spectra of SPC3 (solid line), $[GPGQAF]_8$-SPC (circle), $[IGPGRAF]_8$-SPC (diamond), $[GPGRA]_8$-SPC (triangle), and $[GPGR]_8$-SPC (square) in 20 mM phosphate buffer, pH 7 (panel A), and in a water solution containing 50% trifluoroethanol (panel B).

B CD spectrum (a weak negative band between 220 and 230 nm, a positive band between 200 and 210 nm, and a strong negative band between 180 and 190 nm) usually associated to type II β-turn, while SPC3 in TFE shows a class C CD spectrum (a weak negative band at about 220 nm, a negative band between 200 and 210 nm, and a positive band between 180 and 195 nm) usually associated to type I β-turn (Woody, 1985; Perczel et al., 1993; Baldwin et al., 1994). In phosphate buffer, pH 7, the monomer has a class B CD spectrum, while SPC3 has a negative band at 200 nm associated to random coil structure (Johnson, 1985) and another negative band at 185 nm frequently found in β-turn CD spectra (Brahms & Brahms, 1980). There are different conformational types of β-turns based on the ψ and ϕ angle values, and the denoted type I and type II β-turns constitute 80% of the β-turns described in proteins (Wilmot & Thornton, 1988). The main difference between type I and type II is an inversion of the plane of the peptide bond between $i + 1$ and $i + 2$. To investigate the effect due to the polymerization, analogs were synthesized with two and four motifs. In TFE, their CD spectra are different from class B and C spectra (Figure 1B). Our interpretation is that these CD spectra correspond to a conformational equilibrium between type I and type II β-turns. These results indicate a different structure for the GPGRAF motif in the V3 loop and in SPC3, and these structural changes are correlated to the degree of polymerization.

SPC3 analogs with eight motifs were synthesized differing from the GPGRAF sequence (Table 1). The SPC analog $[IGPGRAF]_8$-SPC has a CD spectrum similar to that of SPC3 at pH 7 (Figure 2A) and in TFE (Figure 2B); nevertheless in TFE there is UV shift for the positive band at 190 nm. The $[GPGR]_8$-SPC, $[GPGRA]_8$-SPC, and $[GPGQAF]_8$-SPC spectra are markedly different from the SPC3 spectra at pH 7 and in TFE. At pH 7, they have a negative band at 200 nm as SPC3, but there is no negative band at 185 nm in these three analogs (Figure 2A). In TFE, these spectra are different from either the class B or class C spectrum (Figure 2B). $[GPGKTL]_8$-SPC and $[RAFVTIGK]_8$-SPC have CD spectra similar to that of $[GPGRA]_8$-SPC (data not shown). These results show that the SPC3 structure stability is tightly correlated to at least the GPGRAF sequence.

A cell-to-cell assay based on the fusion between the CEM-derived cell clone 8E5, chronically infected with HIV-1 (IIIB), and PHA-stimulated human PBMCs was used to evaluate the antifusion activity of SPC3 and analogs. Table 1 shows that polymerization of the GPGRAF motif in the eight-branched construction resulted in the creation of an

Table 1: Inhibition of HIV-1-Induced Cell Fusion by SPCs[a]

peptides	concn inhibiting syncytia formation by 100%	secondary structure in TFE
GPGRAF (monomer)	$\gg 50\ \mu M$[b,d]	type II β-turn
$[GPGRAF]_2$-SPC	$50\ \mu M$	type I and II β-turns
$[GPGRAF]_4$-SPC	$50\ \mu M$	type I and II β-turns
[GPGRAF]8-SPC	**5 μM**[c]	type I β-turn
$[IGPGRAF]_8$-SPC	$50\ \mu M$[c]	type I β-turn
$[GPGRA]_8$-SPC	$\gg 50\ \mu M$[c]	other[e]
$[GPGR]_8$-SPC	$\gg 50\ \mu M$[c]	other[e]
$[RAFVTIGK]_8$-SPC	$\gg 50\ \mu M$[c]	other[e]
$[GPGKTL]_8$-SPC	$\gg 50\ \mu M$	other[e]
$[GPGQAF]_8$-SPC	$\gg 50\ \mu M$	other[e]

[a] HIV-1-expressing cells chronically infected with a RT-deficient HIV-1 (IIIB) isolate were cocultivated with PHA-stimulated PBMCs in the presence of the indicated peptide at various concentrations up to 50 μM, as described in Materials and Methods. The number of syncytia was determined after 24 h of incubation in the continued presence of the peptides. [b] According to Fantini et al. (1993). [c] According to Yahi et al. (1994). [d] No effect observed at 50 μM. [e] Other means structures that are not α-helix, β-turn, or β-sheet.

Table 2: β-Turn Types Observed with the Gly-Pro-Gly Sequence within the Protein Data Bank[a]

protein	sequence	position $i+1$		position $i+2$		β-turn type
		$\phi°$	$\psi°$	$\phi°$	ψ	
adenylate kinase	GPGS	−63.9	129	85.4	0	II
mengo encephalomyocarditis virus coat protein	GPGT	−70.2	−25	−108.2	23.2	I
rhodanese	GPGL	−46.7	−11	−87	−79.7	undetermined
satellite tabacco necrosis virus	GPGA	−59	116.4	114.9	−1.7	II
wheat germ agglutinin	GPGY	−55.5	−45.1	−60.4	−36.9	I

[a] Bernstein et al., 1977.

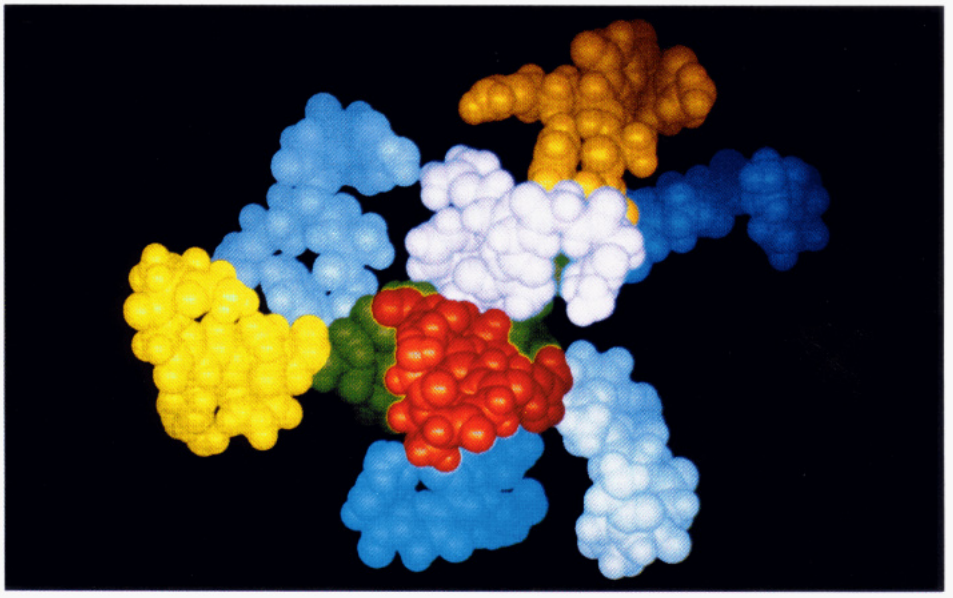

FIGURE 3: SPC3 model. The model was build with Insight II and Discover from BIOSYM Technologies, Inc. (San Diego, CA), running on a Silicon Graphics XS 24 R3000 Indigo Workstation. SPC3 is made of a β-alanine and seven lysine residues colored in green connecting together eight GPGRAF motifs represented with specific colors. The structures were optimized in vacuum with the CVFF force field in terms of the internal energies, using the van der Waals energy to monitor each step of the modeling. The pH was set up at 7. Minimization was performed with steepest descent, conjugate gradient, and quasi Newton Raphton algorithms with a maximum derivative of 0.1 kcal in the final steps. Dynamic steps were performed at 300 K.

antiviral activity. In order to determine what should be the minimal degree of polymerization to get this activity, GPGRAF SPCs with two and four branches were evaluated in this cell-to-cell assay. The results showed that both derivatives had some activity in this test but none of them were as active as SPC3. Next, the activity of eight-branched SPCs with variations of the size and sequence of the GPGRAF motif was tested. The effect was highly specific and dependent on the sequence of the motif since $[GPGQAF]_8$-SPC and $[GPGKTL]_8$-SPC were not active in this assay. SPCs with less than six residues, i.e., $[GPGRA]_8$-SPC or $[GPGR]_8$-SPC, did not inhibit cell fusion. Addition of the highly conserved isoleucine residue at the N-terminal part of the motif (i.e., IGPGRAF) resulted in a significant loss of activity in comparison with SPC3 (Yahi et al., 1994). Comparison of the activity test and CD spectra shows that SPC3 and the active analogs ($[GPGRAF]_2$-SPC, $[GPGRAF]_4$-SPC, and $[IGPGRAF]_8$-SPC) have similar CD spectra at pH 7 (Figure 1A,B). In TFE, $[IGPGRAF]_8$-SPC is the only octamer analog to have a CD spectrum similar to SPC3. $[GPGRAF]_2$-SPC and $[GPGRAF]_4$-SPC probably correspond to a conformational equilibrium between type I and type II β-turns, and their lower activity in regard to SPC3 (Table 1) could be explained by the impossibility for these derivatives to adopt a full type I β-turn conformation. Taken together, the data suggest that there is a correlation between the structure of the peptide in a type I β-turn and an antiviral activity. However, since $[IGPGRAF]_8$-SPC has a lower activity in regard to SPC3, the N-terminal extremity could play also a role in the SPC3 activity. This is confirmed by the derivative $[Ac\text{-}GPGRAF]_8$-SPC that has the N-terminus acetylated and a lower activity compared to SPC3 (Yahi et al., 1994).

The gp120 V3 loop was predicted to assume a β-strand−type II β-turn−β-strand-α helix conformation with a turn at GPGR (La Rosa, 1990). A β-turn structure for the sequence GPGR is shown by 2D nuclear magnetic resonance (NMR) of 20 residue long peptides from the V3 loop where this structure is conserved both in aqueous solution and in the presence of TFE; no NMR data were available to determine the β-turn type because of the presence of a proline in $i+1$ (Zvi et al., 1992). On the other hand, the crystal structure of the complex made from an antibody fragment and a V3 loop peptide shows that the GPGR sequence adopts a type II β-turn (Ghiara et al., 1994). This is a confirmation of the interpretation of our CD data for the monomer. The analysis of 59 nonhomologous proteins (Wilmot & Thornton, 1988) shows that Gly is found at the i position mainly for a type I β-turn, while Pro is the most frequent amino acid residue at position $i+2$ in type I and II β-turns. However, Gly is highly favored at the $i+2$ position, and there is a significant probability to have Arg at the $i+3$ position for type II β-turns. The Protein Data Bank (Bernstein et al., 1977) was used to find the sequence Gly-Pro-Gly-X in the β-turn

structure. Although the motif Gly-Pro-Gly is found in 15 proteins, only 5 are in the β-turn structure. Among these five β-turns, two are identified as type I β-turn and two as type II β-turn, and one belongs to a different type. Table 2 shows that the Gly-Pro-Gly sequence can be found in type I as well as in type II β-turns and has no particular propensity to form a type II β-turn structure.

Two SPC3 models were built with the eight GPGR sequences either in type I or in type II β-turns, Ala and Phe being modeled in extended structure to allow the binding to the polylysine backbone. Energy minimization and dynamic steps in vacuum were used for both models. The SPC3 type I β-turn model showed a spreading of the eight GPGRAF sequences around the polylysine backbone (Figure 3). The SPC3 type II β-turn model showed a similar tendency with the major difference that the type II β-turn structure of the GPGR sequences disappeared during minimization to adopt a random structure (data not shown). These calculations show that the type II β-turn structure for the GPGR sequence is not favored in the SPC3 model, while the type I β-turn structure remains unchanged after energy minimization and dynamic steps. It was not possible to get a SPC3 model with a type I β-turn from a starting model having a type II β-turn or other structures. The solvent may probably play a determinant role in the GPGR structure in the type I β-turn.

A ligand design study was made with the software LUDI from BIOSYM (San Diego, CA) to determine the possible interaction of the GPGRAF motif with amino acid side chains. Two researches were made with the sequence in the type I and type II β-turn. The search area was reduced to a sphere of 10 Å centered on the proline Cα. The ligand research was done exclusively with the amino acid side chain, and the rules governing the generation of interaction were according to Taylor and Kennard (1984). The data show that GPGR in a type I β-turn constitutes a proton acceptor pair fitting with the H-donor doublet of an arginine side-chain extremity. In contrast, no specific interaction was found with any amino acid side chain for GPGR in a type II β-turn.

In conclusion, our data show that there is a clear relationship between the SPC3 structure and its antiviral activity. The potent antiviral activity of SPC3 correlates with its propensity to achieve a type I—but not a type II—β-turn in solution. Both polymerization and sequence specificity are important to stabilize type I β-turns in SPC3. These data provide a structural basis for the striking antiviral properties of SPC3, which represents a new class of potential anti-HIV candidate therapeutic drugs.

ACKNOWLEDGMENT

We thank Colette Roussarie and Razika Oughideni for technical assistance. We thank Dr. Jean-Marc Sabatier for the generous gift of SPC3 and SPC analogs. We thank Dr. Françoise Guerlesquin for helpful discussion.

REFERENCES

Baldwin, J. E., Claridge, T. D. W., Hulme, C., Rodger, A., & Schofield, C. J. (1994) *Int. J. Pept. Protein Res. 43*, 180−183.

Bernstein, F. C., Koetzle, T. F., Williams, G. J. B., Meyer, E. F., Brice, M. D., Rodgers, J. R., Kennard, O., Shimanouchi, O., & Tasumi, M. (1977) *J. Mol. Biol. 112*, 535−542.

Bolognesi, D. P. (1993) *Adv. Virus Res. 42*, 103−148.

Brahms, S., & Brahms, J. (1980) *J. Mol. Biol. 138*, 149−178.

De Rossi, A., Pasti, M., Mamano, F., Panozzo, M., Dettin, M., Di Bello, C., & Chieco-Bianchi, L. (1991) *Virology 184*, 187−196.

Fantini, J., Yahi, N., Mabrouk, K., Van Rietschoten, J., Rochat, H., & Sabatier, J. M. (1993) *C. R. Acad. Sci., Ser. 3 316*, 1381−1387.

Folks, T., Benn, S., Rabson, A., Theodore, T., Hoggan, M. D., Matrin, M., Lightfoot, M., & Sell, K. (1985) *Proc. Natl. Acad. Sci. U.S.A. 82*, 4539−4543.

Ghiara, J. B., Stura, E. A., Stanfield, R. L., Profy, A. T., & Wilson, I. A. (1994) *Science 264*, 82−85.

Hildreth, J. E., & Orentas, R. J. (1989) *Science 244*, 1075−1078.

Hwang, S. S., Boyle, T. J., Lyerly, H. K., & Cullen, B. R. (1991) *Science 253*, 71−74.

Javaherian, K., Langlois, A. J., LaRosa, G. J., Profy, A. T., Bolognesi, D. P., Herlihy, W. C., Putney, S. D., & Matthews, T. J. (1990) *Science 250*, 1590−1593.

Johnson, W. C., Jr. (1985) *Methods Biochem. Anal. 31*, 61−163.

LaRosa, G. J., Davide, J. P., Weinhold, K., Waterbury, J. A., Profy, A. T., Lewis, J. A., Langlois, A. J., Dreesman, G. R., Boswell, R. N., Sadduck, P., Holley, L. H., Karplus, M., Bolognesi, D. P., Matthews, T. J., Emini, E. A., & Putney, S. D. (1990) *Science 249*, 932- 935.

Merrifield, R. B. (1986) *Science 232*, 341−347.

Moore, J. P., & Nara, P. L. (1991) *AIDS 5*, S21−S33.

Nardelli, B., Lu, Y. A., Shiu, D. R., Dempierre-Defoort, C., Profy, A. T., & Tam, J. P. (1992) *J. Immunol. 148*, 914−920.

Nehete, P. M., Arlinghaus, R. H., & Sastry, K. J. (1993) *J. Virol. 67*, 6841−6846.

Perczel, A., Hollosi, M., Sandor, P., & Fasman, G. (1993) *Int. J. Pept. Protein Res. 41*, 223−236.

Sabatier, J. M., Zerrouk, H., Darbon, H., Mabrouk, K., Benslimane, A., Rochat, H., Martin-Eauclaire, M. F., & Van Rietschoten, J. (1993) *Biochemistry 32*, 2763−2770.

Tam, J. P. (1988) *Proc. Natl. Acad. Sci. U.S.A. 85*, 5409−5413.

Taylord, R., & Kennard, O. (1984) *Acc. Chem. Res. 17*, 320−329.

Urry, D. W. (1972) *Biochim. Biophys. Acta 265*, 115−168.

Wilmot, C. M., & Thornton, J. M. (1988) *J. Mol. Biol. 203*, 221−232.

Woody, R. W. (1985) in *Peptides* (Hruby, V. J., Ed.) Vol. 7, pp 38−40, Academic Press, New York.

Yahi, N., Fantini, J., Hirsch I., & Chermann, J. C. (1992) *Arch. Virol. 125*, 287−298.

Yahi, N., Fantini, J., Mabrouk, K., Tamalet, C., de Micco, P., Van Rietschoten, J., Rochat, H., & Sabatier, J. M. (1994) *J. Virol. 68*, 5714−5720.

Zvi, A., Hiller, R., & Anglister, J. (1992) *Biochemistry 31*, 6972−6979.

BI9428641